Two Fundamental Mechanisms Govern the Stiffening of Cross-linked Networks

Goran Žagar[†], Patrick R. Onck[†] and Erik van der Giessen[†*]

[†]Zernike Institute for Advanced Materials, University of Groningen, Groningen,The Netherlands

SUPPLEMENTARY MATERIAL

Network generation

Random networks are generated by starting from a collection of straight fibers of length l_0 that are randomly positioned and oriented within a periodic box of size W^3. The number of filaments in the box, n_f, is determined by the desired concentration $c_\mathrm{f} = \rho_\mathrm{f}(t/2)^2\pi n_\mathrm{f} l_0/W^3$, where ρ_f and t are the intrinsic filament density and diameter, respectively.

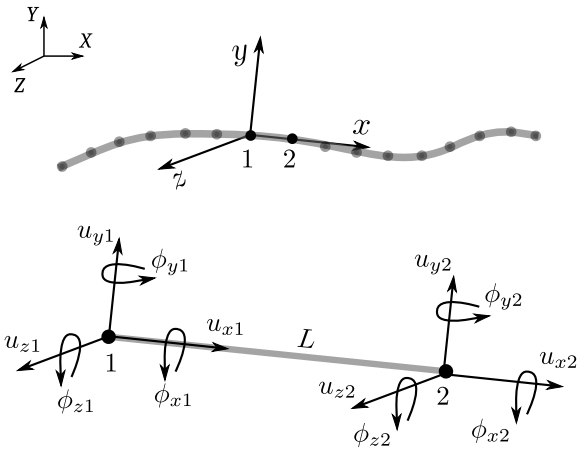

FIGURE S1 Fibers are discretized into two-node beam elements. Each node of a beam element in 3D has 6 degrees of freedom. Every beam element has a local coordinate system (x, y, z), while (X, Y, Z) are global coordinates.

All fibers are discretized into 3D beam (finite) elements that can stretch, bend and twist (Figure S1). The vectors of nodal displacements and loads of a beam element in a local coordinate system (x, y, z) are defined as

$$\mathbf{u} = \left\{u_{x1}, u_{y1}, u_{z1}, \ell\phi_{x1}, \ell\phi_{y1}, \ell\phi_{z1}, u_{x2}, u_{y2}, u_{z2}, \ell\phi_{x2}, \ell\phi_{y2}, \ell\phi_{z2}\right\}^\mathrm{T} \tag{S1}$$

and

$$\mathbf{f} = \left\{f_{x1}, f_{y1}, f_{z1}, \frac{m_{x1}}{\ell}, \frac{m_{y1}}{\ell}, \frac{m_{z1}}{\ell}, f_{x2}, f_{y2}, f_{z2}, \frac{m_{x2}}{\ell}, \frac{m_{y2}}{\ell}, \frac{m_{z2}}{\ell}\right\}^\mathrm{T}, \tag{S2}$$

0006-3495/08/09/2624/12 $2.00 doi: 10.1529/biophysj.106.090944

respectively, where ℓ is an arbitrary length. The constitutive behaviour of a beam element is described in terms of the linear relation $\mathbf{s}_\mathrm{e} = \mathbf{S}_\mathrm{e}\mathbf{e}_\mathrm{e}$ (generalised Hooke's law) between the generalized stress and strain defined as,

$$\mathbf{s}_\mathrm{e} = \begin{Bmatrix} f_{\mathrm{x}2} \\ f_{\mathrm{y}1} \\ f_{\mathrm{z}2} \\ \frac{m_{\mathrm{x}2}}{L} \\ \frac{m_{\mathrm{y}2}}{L} \\ \frac{m_{\mathrm{z}2}}{L} \end{Bmatrix} \quad \text{and} \quad \mathbf{e}_\mathrm{e} = \begin{Bmatrix} u_{\mathrm{x}2} - u_{\mathrm{x}1} \\ u_{\mathrm{y}1} - u_{\mathrm{y}2} + L\phi_{\mathrm{z}1} \\ u_{\mathrm{z}2} - u_{\mathrm{z}1} + L\phi_{\mathrm{y}1} \\ (\phi_{\mathrm{x}2} - \phi_{\mathrm{x}1})L \\ (\phi_{\mathrm{y}2} - \phi_{\mathrm{y}1})L \\ (\phi_{\mathrm{z}2} - \phi_{\mathrm{z}1})L \end{Bmatrix}, \tag{S3}$$

respectively. Application of Euler-Bernoulli beam theory leads to the well-known stiffness matrix

$$\mathbf{S}_\mathrm{e} = \begin{bmatrix} \frac{\mu}{L} & 0 & 0 & 0 & 0 & 0 \\ 0 & 12\frac{\kappa}{L^3} & 0 & 0 & 0 & 6\frac{\kappa}{L^3} \\ 0 & 0 & 12\frac{\kappa}{L^3} & 0 & 6\frac{\kappa}{L^3} & 0 \\ 0 & 0 & 0 & \frac{\tau}{L^3} & 0 & 0 \\ 0 & 0 & 6\frac{\kappa}{L^3} & 0 & 4\frac{\kappa}{L^3} & 0 \\ 0 & 6\frac{\kappa}{L^3} & 0 & 0 & 0 & 4\frac{\kappa}{L^3} \end{bmatrix}, \tag{S4}$$

where μ, κ and τ are the axial, the bending and the torsional stiffness, respectively, and L is the element length. The elastic properties of the elements in Eq. S4 are chosen such that they mimic semiflexible filaments.

The system of discretized fibers starts to move and distort due to a weak $1/r^2$ attractive force field that is introduced between any two uncross-linked nodes of two different fibers. This field exerts an attractive force between nodes i and j given by $f_\mathrm{p}^{ij} = f_0 m^{ij}(r_0/r^{ij})^2$, where f_0 is the force magnitude parameter, r^{ij} is the distance between the two nodes and $m^{ij} = (m^i m^j)/m_0^2$ is the mass of two nodes relative to their initial mass, $m_0 = \rho_\mathrm{f}(t/2)^2\pi L/2$. The force field has a cut-off r_0 so that $f_\mathrm{p}^{ij} = 0$ for $r^{ij} > r_0$. The motion is assumed to take place in a fluid environment (water) characterized by a viscosity η, yet thermal fluctuations are ignored. Note that by ignoring thermal fluctuations, we are not accounting for the entropic part of the fiber free energy. An additional internal damping of the fibers is added for numerical convenience, so that the natural vibrational modes of the fibers are somewhat overdamped. Thus, with the vector of nodal velocities and accelerations denoted by $\dot{\mathbf{u}}$ and $\ddot{\mathbf{u}}$, respectively, the equation of motion for a beam element reads

$$\mathbf{m}\ddot{\mathbf{u}} = \mathbf{f}_\mathrm{p} - (\mathbf{f}_\mathrm{v} + \mathbf{f}_\mathrm{i}) - \mathbf{f}_\mathrm{e}, \tag{S5}$$

where $\mathbf{m}$ is the diagonally lumped mass matrix, $\mathbf{f}_\mathrm{p}$ is the resultant force vector of nodal interactions, $\mathbf{f}_\mathrm{v}$ and $\mathbf{f}_\mathrm{i}$ are the nodal drag force vectors due to viscous effects and internal damping, respectively, and $\mathbf{f}_\mathrm{e}$ is the nodal elastic force vector. After transformation to the global frame of reference(X,Y,Z) coordinates, the element eqs. S5 are assembled into a general system of equations that is subsequently solved for all nodal displacements and integrated in time adopting the velocity Verlet algorithm with simultaneous updating of the element orientations and deformations (in the spirit of an Updated Lagrangian scheme).

All networks used here are generated with the same force field parameters. The force field parameters are chosen to be weak enough so as to allow for gentle network self-assembly while avoiding the collapse of the fibers into heterogeneous structures predominately made from fiber bundles. During the generation procedure, if two nodes of two different fibers come closer than some threshold distance, they are connected by a rigid cross-link. Each cross-link is allowed to join only a single pair of different fibers. As the dynamics proceeds, the number of cross-linked fibers increases and multiple cross-links partition a fiber into a number of sections. The assembly process is halted once the desired mean length of fiber sections, l_c, is reached. Although the generated networks are internally pre-stressed, this is neglected and subsequently all network sections are straightened-out, while mechanically irrelevant dangling ends and disconnected clusters are removed from the network. The generated microstructure of the RVE can be varied through the input triplet $(c_\mathrm{f}; l_0; l_\mathrm{c})$. Even though all fibers have the same initial length, the distribution of section lengths is exponential, see Fig. S2, just like those predicted by molecular dynamics simulations (1).

Network deformation

Simulations of the network deformation are conducted in a quasi-static manner, i.e., during computation of a network response the inertial and all damping terms in Eq. S5 are ignored. In addition, we assume that the liquid constituent is incompressible and at rest during deformation so that the change of the RVE volume is controlled mainly by the bulk modulus of the liquid.

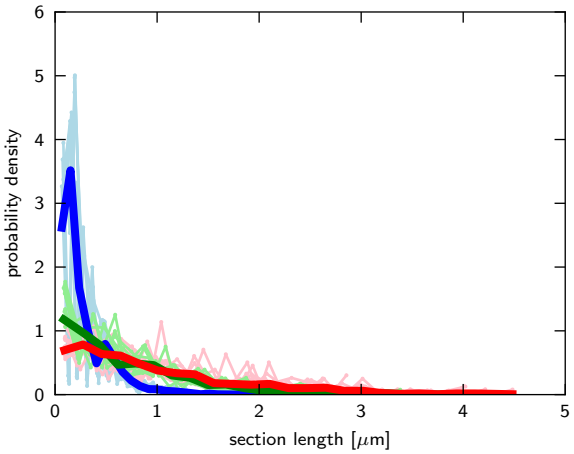

FIGURE S2 Probability density function of the section lengths (thick lines) in generated networks with fiber concentration $c_f = 0.8$ mg/mL and initial fiber length $l_0 = 5\mu$m having a mean section length $l_c \approx 1.2$ (red), 0.86 (green) and 0.34 μm (blue). The ensemble distributions are obtained from 10 network realizations for each l_c as a single data set (the distribution for each realization is plotted with thin lines in light color to indicate the scatter). The number of bins for every distribution is 25.

However, in simple shear, the volume of the RVE remains constant and the work of hydrostatic pressure is zero. The governing incremental equation for a beam element is then simply $\Delta\mathbf{f}_e = \mathbf{K}_e\Delta\mathbf{u}$.

Cross-links are modeled as linear springs whose behaviour is represented by the simple diagonal stiffness matrix,

$$\mathbf{S}_{cl} = \begin{bmatrix} s_1 & 0 & 0 & 0 & 0 & 0 \\ 0 & s_3 & 0 & 0 & 0 & 0 \\ 0 & 0 & s_3 & 0 & 0 & 0 \\ 0 & 0 & 0 & s_4 & 0 & 0 \\ 0 & 0 & 0 & 0 & s_2 & 0 \\ 0 & 0 & 0 & 0 & 0 & s_2 \end{bmatrix}, \tag{S6}$$

where spring constants s_1, s_2, s_3 and s_4 are defined in Figure 2B in the main text. Similarly as for the beam elements, the incremental cross-link element law can be expressed in terms of nodal force and displacement increments, $\Delta\mathbf{f} = \mathbf{K}_{cl}\Delta\mathbf{u}$, where $\mathbf{K}_{cl}$ is the now the cross-link element stiffness matrix.

The incremental equations for all beam and cross-link elements are assembled into a system of equations that, subject simple shear boundary conditions, is solved for the nodal displacement and force increments in global coordinates. Large deformations of the RVE are obtained by adopting an Updated-Lagrangian scheme.

Energy partitioning during deformation of a network with compliant cross-links

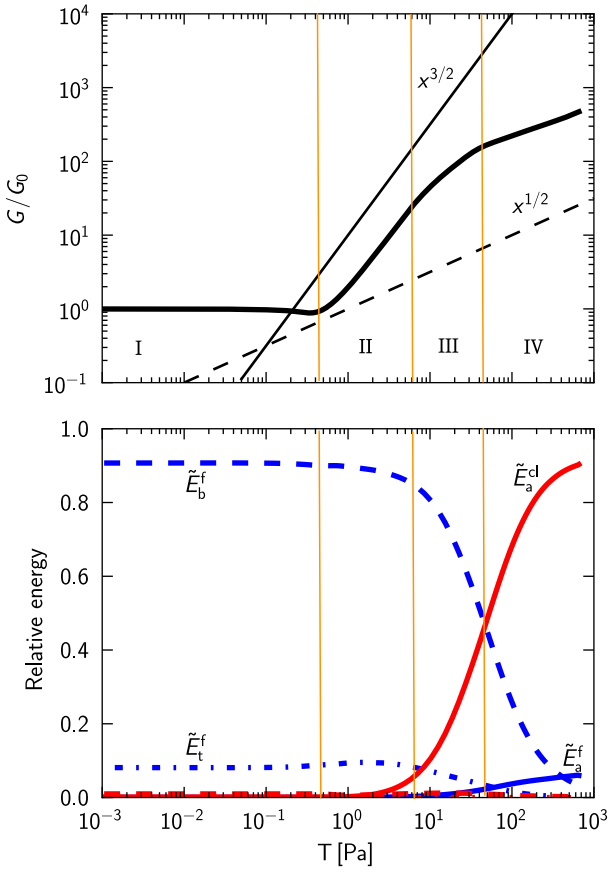

FIGURE S3 Normalized shear modulus G/G_0 (above) and relative energy (below) as a function of shear stress T for a single network realization ($\tilde{n}_X = 0.34$) with fiber properties that represent F-actin and cross-link number $\tilde{s} = 10^4$. Relative axial $\tilde{E}_a$ (solid line), bending $\tilde{E}_b$ (dashed line) and torsional $\tilde{E}_t$ (dash-dotted line) energy for fibers (blue color, superscript "f") and cross-links (red color, superscript "cl") at each stress level is obtained by normalization with respect to the total energy at this stress level, $E_a^f + E_b^f + E_t^f + E_a^{cl} + E_b^{cl} + E_t^{cl}$. The two stiffening mechanisms divide network response into four parts: (I) constant G/G_0, (II) bending 3/2 stiffening region, (III) bending-to-stretching transition region and (IV) stretching 1/2 stiffening region.

Stress path in a box

The nonlinear behavior of a network containing a stiffening stress path as that of a single fiber of filament sections and cross-links in a cubic box of length W, as shown in Fig. 4 in the main text. Beyond the critical strain level Γ_c with corresponding critical stress T_c, the initial stiffness G_0 changes abruptly into a stiffness that depends on the relative strain $\gamma := \Gamma - \Gamma_c$. In order to derive this function $G(\gamma)$, we consider continued shearing by an infinitesimal amount $d\Gamma = du/W$. The associated displacement increment du requires the end-to-end vector of this stress path to increase by an amount dr and to simultaneously rotate. By simple geometrical considerations, see Fig. S4, these incremental changes are connected by $dr = du \sin\beta$.

The change of length dr requires an increase of the end-to-end force, df_r, which will be a function of the end-to-end distance r and the constitution of the stress path. Since, by construction, the stress path is the only load bearing structure, the component $df_x = df_r \sin\beta$ in the shearing direction determines the change in overall shear stress T as $dT = df_x/W^2$. Putting

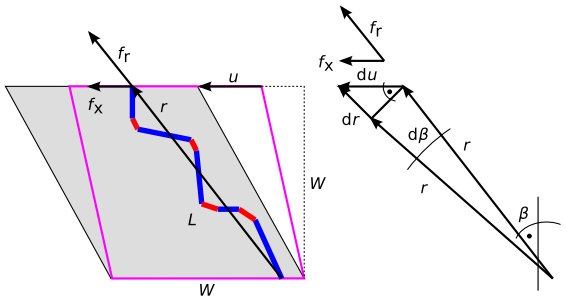

FIGURE S4 Simple shear of the box containing a percolating stress path. The box at the critical point is shown in magenta. Fiber constituents are shown in blue, and cross-links in red.

all this together, we find that the instantaneous stiffness satisfies

$$G = \frac{\mathrm{dT}}{\mathrm{d}\Gamma} \propto \frac{\mathrm{d}f_\mathrm{r}}{\mathrm{d}r} \sin^2\beta \tag{S7}$$

Interesting scaling relations between G and γ can be found by considering two limiting situations.

The first limiting case is the RCL network, as already put forward in (2). Such a network stiffens so rapidly that $\gamma \approx 0$ and β remains roughly constant at the critical value β_c. As a consequence, $G \propto \mathrm{d}f_\mathrm{r}/\mathrm{d}r$ from Eq. S7. The stress path in this case consists of an athermal yet undulated filament, which rapidly stiffens when its length r approaches its contour length L. In fact, (3), the force f_r in inextensible filaments diverges as $(L-r)^{-2}$ when $r \to L$. Hence, $G \propto (L-r)^{-3}$ or $G \propto \mathrm{T}^{3/2}$. The stiffness of extensible filaments does not diverge but is limited by the axial stiffness μ. Thus, $G \propto \mu$ defines an upper limit to the validity of the above $3/2$ scaling law, (2).

On the other hand, when the cross-link compliance is significant, networks are more easily deformed to larger strains and the reorientation of the stress path during stiffening can be substantial. In this case, the response beyond the critical point is linear and controlled by the cross link stiffness s, as observed in Fig. 3G. With $\mathrm{d}f_\mathrm{r}/\mathrm{d}r \propto s$, what remains is to find the relationship between $\sin^2\beta$ and γ. For the purpose of arriving at a simple form, we will consider small excursions into the nonlinear regime, so that $\beta - \beta_\mathrm{c}$ is small. Then, we set $\cos\beta \approx \cos\beta_\mathrm{c}$ so that $\sin\beta$ can be developed as $\sin\beta = \tan\beta\cos\beta_\mathrm{c} = (\tan\beta_\mathrm{c} + \gamma)\cos\beta_\mathrm{c} = \sin\beta_\mathrm{c} + \gamma\cos\beta_\mathrm{c}$. The two leading terms in the expansion of Eq. S7 thus become

$$G \propto s(\sin^2\beta_\mathrm{c} + \gamma \sin 2\beta_\mathrm{c})\,. \tag{S8}$$

Writing the bracketed term as $y = a + b\gamma$, with a and b being constants, we find that $G = \mathrm{dT}/\mathrm{d}\Gamma = \mathrm{dT}/\mathrm{d}\gamma = \mathrm{dT}/\mathrm{d}y$ leads to the differential equation $\mathrm{dT} \propto s y \mathrm{d}y$. Its solution $\mathrm{T} \propto s y^2$ allows us to write $G \propto y$ or $G \propto \mathrm{T}^{1/2}$ for cross-link dominated stiffening.

According to the derivation above, a power-law dependence of the instantaneous modulus on stress with exponent $1/2$ is expected when the nonlinear strain γ is small enough that the dependence of the re-orientation of the stress path on γ is linear. Nonlinear effects at large strains are expected to push the exponent away from $1/2$ towards a constant stiffness of $G \propto s$.

REFERENCES

1. Kim, T., W. Hwang, H. Lee, and R. D. Kamm, 2009. Computational Analysis of Viscoelastic Properties of Crosslinked Actin Networks. PLoS Comput. Biol. 5:e1000439.
2. Žagar, G., P. R. Onck, and E. Van der Giessen, 2011. Elasticity of Rigidly Cross-Linked Networks of Athermal Filaments. Macromolecules 44:7026–7033.
3. Van Dillen, T., P. R. Onck, and E. Van der Giessen, 2008. Models for stiffening in cross-linked biopolymer networks: A comparative study. J. Mech. Phys. Solids 56:2240–2264.

List of Figures